Available online at www.sciencedirect.com
SCIENCE DIRECT
Journal of Membrane Science 271 (2006) 140–150
journal of MEMBRANE SCIENCE
www.elsevier.com/locate/memsci

Grand canonical Monte Carlo and non-equilibrium molecular dynamics simulation study on the selective adsorption and fluxes of oxygen/nitrogen gas mixtures through carbon membranes

Shu-Mei Wang [a,b], Yang-Xin Yu [a,b,*], Guang-Hua Gao [a,b]

[a] *Department of Chemical Engineering, Tsinghua University, Beijing 100084, PR China*
[b] *State Key Laboratory of Chemical Engineering, Tsinghua University, Beijing 100084, PR China*

Received 8 March 2005; received in revised form 19 June 2005; accepted 10 July 2005
Available online 26 August 2005

Abstract

The equilibrium selective adsorption and fluxes of oxygen/nitrogen binary gas mixtures through carbon membranes are investigated at 303 K, respectively, using a grand canonical Monte Carlo simulation and a dual control volume grand canonical molecular dynamics method. The carbon membrane pores are modeled as slit-like pores with a two-dimensional structure where carbon atoms are placed according to the structure of graphite layers. The effect of the membrane thickness, bulk pressure, and pore width on the equilibrium selective adsorption and dynamic separation factor is discussed. Meanwhile a new iteration approach to calculate the flux and dynamic separation factor of binary gas mixtures through membranes is proposed, by which we can simulate the permeation and fluxes of gases through the membranes in the presence of pressure gradient and consider the effect of pressure and composition of low-pressure side in the meantime. The simulated results show that bulk pressure and membrane thickness have no effect on the equilibrium selectivity, but they have a great effect on the fluxes and dynamic separation factors of gases. The pore width impacts the equilibrium selectivity and dynamic separation factors strongly, especially when the pore width is very small. Molecular sieving dominates the separation of oxygen/nitrogen in non-equilibrium simulations. But due to the comparable molecular size of oxygen and nitrogen, we have to modify the carbon membranes in order to improve dynamic separation of atmosphere.

Keywords: Gas separation; Carbon membrane; Molecular simulation; Adsorption; Flux

1. Introduction

Membrane technology is one of the most competitive supporting-technologies boosting the chemical engineering. Gas separation, as one of the most important membrane processes, has been currently of fundamental and practical interest. Since the air is the cheapest, easily available, and unexhausted source of obtaining both the nitrogen and oxygen as the basic feed gas for industrial applications, air separation using membranes has been well known as the creating-resource technology. Carbon membranes are emerging as promising candidates for air separation applications due to not only their stable thermodynamic and mechanical properties but also their uniform porosity distribution and easily controllable pore size. In this paper, we mainly focus on the characters of adsorption and permeation of N_2/O_2 gas mixture in carbon membranes under the various conditions.

Up to date, many recent molecular simulation studies have carried out on the adsorption [1,2] and transport of some fluids or their mixtures in various inorganic membranes (e.g. carbon [3–7], zeolite [8] and silica gel [9–12]), resulting in a better understanding of the effect of confinements (including pressure, temperature, membrane model, and pore size and shape, etc.) on the behavior of the fluids. Generally, grand canonical

* Corresponding author. Tel.: +86 10 62782558; fax: +86 10 62770304.
E-mail address: yangxyu@mail.tsinghua.edu.cn (Y.-X. Yu).

0376-7388/$ – see front matter © 2005 Elsevier B.V. All rights reserved.
doi:10.1016/j.memsci.2005.07.033

Monte Carlo (GCMC) is adopted to simulate the equilibrium adsorption, while molecular dynamics simulation (MD) is more preferable to study the non-equilibrium transport properties [13]. Recently some non-equilibrium molecular dynamics (NEMD) methods have also been developed, such as the grand canonical molecular dynamics (GCMD) method [4,3,14,15] and the dual-volume GCMD technique (DCV-GCMD) [16,4,17–19]. These work provide us valuable clues to insight into the transport and separation of fluids through a porous medium. However, there are still many difficulties that need to be overcome in order to further approach to the truth of transport and adsorption of fluids in membranes. The first attempt in this aspect is that we use a novel two-dimensional slit pore instead of one-dimensional pore for carbon membranes comparing with the previous work [20–22], in which the classic 10-4-3 potential of Steele [23] was used. The 10-4-3 potential of Steele recognizes the pore walls as the infinite planes and neglects its longitudinal structure in the meantime. It may be reasonable for the study on equilibrium characters of fluids in porous materials, such as selective-adsorption, and dynamical characters in a single nanopore [20–22], but it is unsuitable for those studies on non-equilibrium properties of fluids through a membrane because of the finite membrane thickness and its crucial effect on the transport and separation properties of fluids in the membrane pores. In addition, 10-4-3 potential of Steele cannot probe into those phenomena occurring near the membranes surface, which also strongly influence on membrane performance. In fact, some studies on equilibrium adsorption and transport of gases in nanoporous materials [22] and especially silicate membranes [24,25] with the structure of two-dimensional pores have been made. The second attempt is to try to introduce a novel iteration method in membrane fields, which will be described in detail in Section 2 of this paper. In the previous work [26,5,10,27], those particles in the permeate side were usually removed as soon as they permeated through membranes, i.e. zero pressure ($p^{L} = 0$) for the permeate side. It should be pointed out that this method is very smart and stable in saving computer time. But it neglects the effect of the permeate side pressure and composition on the transport of gas mixtures, which are very important factors for membrane processes in fact. However the iteration method in this paper can solve this problem well. Another advantage of the iteration method is its flexible, by which we can simulate the transport and separation of binary gas mixtures in membranes under various real experimental conditions.

In the present work, we investigate adsorption and transport of O_2/N_2 binary gas mixture in a carbon membrane with slit-like pores of the finite length and width at 303 K. The feed mixture is modeled as air, i.e. mole fraction of oxygen is 0.21 and that of nitrogen is 0.79. Comparing with previous work, we improve the membrane model and develop an iteration method in membrane fields. We hope all of these efforts will contribute to the exploration of the higher selectivity membrane materials for air separation.

2. Membrane model and simulation methods

2.1. Membrane model and simulation box

In a simulation system, we investigate the equilibrium selective adsorption and non-equilibrium transport and separation of N_2/O_2 gas mixture in a carbon membrane with slit-like pores. A schematic representation of the system used in our simulations is shown in Fig. 1(a) and (b), in which the origin of the coordinates is at the center of simulation box and transport takes place along the x-direction in the non-equilibrium simulations. In the equilibrium simulations, the box as shown in Fig. 1(a) is employed, whose size is set as 85.20 nm × 4.92 nm × (1.675 + W) nm in x-, y-, and z-directions, respectively, where W is the pore width, i.e. the separation distance between the centers of carbon atoms on the two layers forming a slit pore. The simulation box is divided into three regions where the chemical potential for each component is the same. The middle region (M-region) represents the membrane with slit pores. The membrane thickness is nL_{cc} (where n is an integer and L_{cc} equal to 0.142 nm). In our simulations we use n = 8, 11, 14, 21, 23, 29, 35, and 44 to investigate the effect of the membrane thickness on the selective adsorption of mixture. Period boundary conditions are employed in all three directions. In the non-equilibrium molecular dynamics simulations in

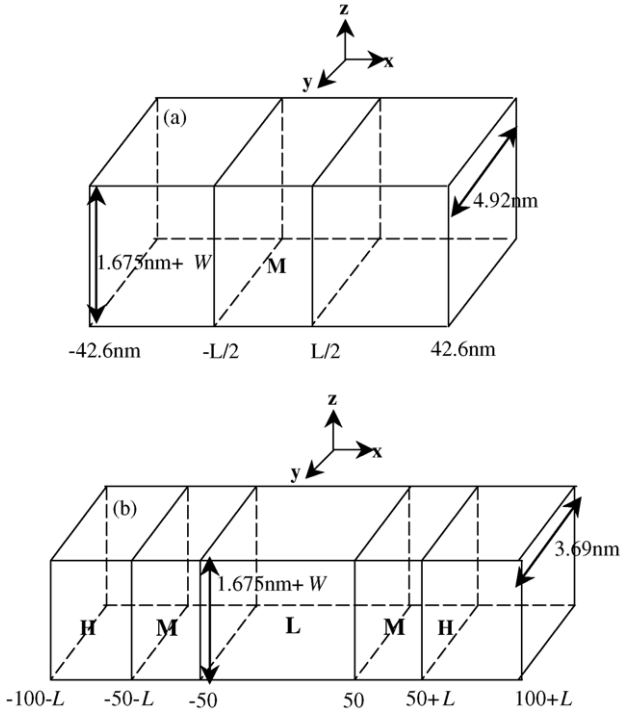

Fig. 1. Schematic representation of the simulation boxes. The H-, L- and M-areas correspond to the high and low chemical potential control volumes, and membrane, respectively. Transport takes place along the x-direction in the non-equilibrium simulations. (a) Equilibrium adsorption simulations and (b) non-equilibrium transport simulations. L is the membrane thickness and W is the pore width.

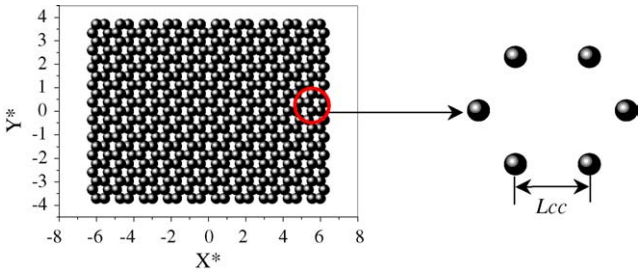

Fig. 2. Planform of one graphic layer. L_{cc} is the separation distance between two adjacent carbon atoms and have a value of 0.142 nm.

order to use period boundary conditions in three directions, we have to divide the system into five regions as shown in Fig. 1(b). The H-regions at the two ends and the L-regions in the middle of the box represent the control volumes (CVs), which correspond to the bulk phase at high and low chemical potential, respectively. The carbon membranes (M-regions) are placed between the two control volumes, i.e. H- and L-regions. The simulated box described above was ever used by Furukawa and Nitta [5]. In non-equilibrium simulations, five pore widths ($W = 2\Delta$, 3Δ, 4Δ, 5Δ and 6Δ) and four membrane thickness ($L = 8L_{cc}$, $11L_{cc}$, $14L_{cc}$ and $17L_{cc}$) are selected to investigate the transport and separation of gas mixtures through carbon membranes, where L_{cc} is the separation distance between two adjacent carbon atoms centers in the same graphite layer ($L_{cc} = 0.142$ nm) and Δ is the separation distance between carbon atom centers of two graphite layers ($\Delta = 0.335$ nm).

The membrane consists of 2232–7380 carbon atoms, which are placed according to the structure of graphite layers (see Fig. 2). There exist six graphite layers between any two slit pores. All the membrane atoms are fixed throughout the simulation process. It is worth to point out that although the pore model used is highly idealized, it is more reasonable to compare with the previous work because besides the pore width, the membrane thickness is considered in our simulations.

We study adsorption and flux of binary mixtures of N_2/O_2. The gas molecules are modeled as Lennard–Jones (LJ) fluid and the interactions between the gas–gas and the gas-carbon atom are modeled with the standard cut-and-shifted LJ 6-12 potential, where the cutoff distance (r_c) was taken to be $5\sigma_{O_2}$, and long-range corrections are not applied, i.e.,

$$V^s(r_{ij}) = \begin{cases} \phi(r_{ij}) - \phi(r_c) & r_{ij} \le r_c \\ 0 & r_{ij} > r_c \end{cases} \quad (1)$$

where r_{ij} is the distance between two particles, and $\phi(r_{ij})$ is the full LJ 12-6 potential

$$\phi(r_{ij}) = 4\varepsilon_{ij}\left[\left(\frac{\sigma_{ij}}{r}\right)^{12} - \left(\frac{\sigma_{ij}}{r}\right)^{6}\right] \quad (2)$$

The values of size parameter σ and energy parameter ε for gases and carbon atom are listed in Table 1. For all the cross-term LJ parameters the Lorentz–Berthelot combining rule is used, i.e. $\varepsilon_{ij} = \sqrt{\varepsilon_i \varepsilon_j}$, and $\sigma_{ij} = (\sigma_i + \sigma_j)/2$. The interaction between a gas molecule and a membrane is obtained by summing over all carbon atoms in the membrane.

Table 1
Values of the LJ parameters used in the simulations

Gas	σ (nm)	ε/k (K)	References
N_2	0.3798	71.4	[31]
O_2	0.3467	106.7	[32]
C	0.34	28.2	[2]

2.2. Equilibrium simulation

A standard grand canonical Monte Carlo (GCMC [13]) simulation is employed in the equilibrium study. Initially, nitrogen and oxygen molecules are randomly placed in the simulation box but the membrane region. Three types of moves are involved in the GCMC simulation: displacement, creation, and deletion. The probabilities of making a displacement, a creation, and a deletion are equal. The chemical potentials, volume and temperature are fixed throughout a whole simulation. The probability of inserting a particle of component i is given by $\hat{P}_i^+ = \min[Z_i V \exp(-\Delta E/kT)/(N_i + 1), 1]$, where $Z_i = \exp(\mu_i/kT)/\Lambda_i^3$ is the absolute activity at temperature T, Λ_i is the de Broglie wavelength, k is the Boltzmann's constant, μ_i is the chemical potential of component i, ΔE is the potential energy change resulting from inserting, deleting or displacing a particle, V is the volume, and N_i is the number of particle i. The probability of deleting a particle of component i is $\hat{P}_i^- = \min[N_i \exp(-\Delta E/kT)/Z_i V, 1]$ and that of displacing a particle of component i is $\hat{P}_i = \min[\exp(-\Delta E/kT), 1]$. Five million configurations are used to reach equilibrium and another 10 million configurations are summed up to get the ensemble average.

For a binary system, the equilibrium separation factor is defined as

$$S = \frac{x_1/y_1}{x_2/y_2} = \frac{\rho^*_{ev1}\rho^*_{b2}}{\rho^*_{ev2}\rho^*_{b1}} \quad (3)$$

where x refers to the adsorption mole fraction, y is the bulk mole fraction, ρ^*_b is the bulk reduced density and ρ^*_{ev} is the average equilibrium density. The subscripts 1 and 2 refer to oxygen and nitrogen, respectively. The average equilibrium density ρ^*_{ev} in the slit and on the membrane surface is, respectively, given by

$$\rho^*_{ev} = \frac{1}{A}\int_A \rho^*(x, z)\,dA \quad (4a)$$

$$\rho^*_{ev} = \frac{1}{L_x}\int_{L_x} \rho^*(x)\,dx \quad (4b)$$

where A is the integrating area of the pore, L_x is the integrating length in x-direction. Eqs. (4a) and (4b) are used to calculate the equilibrium separation factors in the pore and on the membrane surface, respectively. The equilibrium separa-

tion factor is one of the important parameters to describe the selectivity of membrane. The membrane-surface phenomena are as significant as those in the pores for a membrane process. If the membrane surface has a high selectivity for a certain species, the component will enter membrane pores more easily under a given driving gradient. The study on the surface separation factor will give us insights into the modification of membrane surface and membrane materials. We class the separation factor into surface separation factor and that in the pore in the equilibrium simulations although this classification has no significance for a dynamic membrane separation process.

2.3. Non-equilibrium simulation

The GCMD method has recently been used to investigate pressure-driven and chemical potential-driven gas transport through porous inorganic membrane [14,5,4,12]. GCMD combines molecular dynamics (MD) with GCMC methods. The unit cell used in this study is shown in Fig. 1(b). In the MD simulations the velocity Verlet algorithm is used to integrate the equations of motion, for which an adjustable (dimensionless) time step of $t^* = 0.005$ (for wider pore) or 0.003 (for smaller pores) is sufficient to obtain accurate results. To maintain iso-kinetic conditions, the velocity is rescaled independently in all the three directions. To maintain the chemical potentials in the H- and L-regions the GCMC cycles in CVs, incorporating the insertion and deletion of particles, are followed by a series of MD moves for particles through all the regions. Here probabilities of inserting and deleting a particle of component i are the same as those in equilibrium simulations. When a particle is inserted in a CV, it is assigned a thermal velocity selected from the Maxwell–Boltzmann distribution at the given temperature T. An important parameter of the simulations is the ratio R of the number of GCMC cycles in each CV to the number of MD steps. This ratio must be chosen appropriately in order to maintain the correct density and chemical potentials in the CVs, and also reasonable transport rates. In the simulations reported here, the ratio $R = 40{:}1$ for the binary mixtures is adopted.

It should be pointed out that in the industrial membrane process the composition in the permeate side is different from that in the feed side and also changes with operating conditions, namely, the purity of permeated gas is a function of the total pressure ratio $p^{\mathrm{H}}/p^{\mathrm{L}}$, dynamic separation factor S, and composition in feed side. This simple expression [28] is given by:

$$\frac{y}{1-y} = S\frac{p^{\mathrm{H}}x - p^{\mathrm{L}}y}{p^{\mathrm{H}}(1-x) - p^{\mathrm{L}}(1-y)} \tag{5}$$

where x and y are the mole fractions of component 1 in the high and low pressure sides, respectively. S is the separation factor, and p^{H} and p^{L} are the pressures in the high and low pressure sides, respectively. We can also deduce another expression for separation factor from its definition, i.e.,

$$S_{1/2} = \frac{P_1}{P_2} = \frac{\frac{J_1}{J_2}}{\frac{p^{\mathrm{H}}x - p^{\mathrm{L}}y}{p^{\mathrm{H}}(1-x) - p^{\mathrm{L}}(1-y)}} \tag{6}$$

where P_1 and P_2 are the permeability of gas 1 and gas 2, respectively, and J_1 and J_2 are the fluxes of gas 1 and gas 2, respectively. Comparing Eqs. (5) with (6), we can obtain the following equation:

$$\frac{y}{1-y} = \frac{J_1}{J_2} \tag{7}$$

This expression indicates that a certain y has a pair of corresponding J_1 and J_2. If they are introduced into Eqs. (5) and (6), the separation factor from y should be equal to that from J_1 and J_2.

But in all of the previous work about separation of binary mixtures through membranes, a chemical potential gradient is directly given to calculate the flux of components and then to obtain the dynamic separation factor from permeability. As we know, chemical potentials of gas mixture are correlated with their composition at given temperature and pressure, and it is very difficult to measure their values in engineering applications. Therefore results simulated by this way are hardly compared with experimental results. Although in some previous papers [3] pressure gradient is also used as driven force of components transport in membranes, no one gives the method to deal with the relation of y, S and J_1/J_2.

In order to solve this difficulty, in this paper we at first obtain the relation of chemical potentials of species and total pressure and composition by the Widom test particle method that will be described in details as follows. And then a reasonable value of y or separation factor will be obtained by an iteration method. The iterative processes are described as follows:

(i) Give an initial value of y.
(ii) Carry out some certain GCMD steps to obtain the corresponding J_1/J_2.
(iii) Introduce the value of J_1/J_2 into Eq. (7) to calculate a new y'.
(iv) Judge whether y is equal to y'. If not, renew y and the program will start again from the step (ii). The program will stop until difference between y and y' is less than a certain number value.

For each component i we calculate its flux J_i by measuring the net number of its particles in the CVs [16]:

$$J_i = \frac{N_i^{\mathrm{H}} - N_i^{\mathrm{L}}}{2A_{yz}n_{\mathrm{s}}\Delta t} \tag{8}$$

where N_i^{H} and N_i^{L} are the net number of species i added in control volumes. The superscripts H and L represent the high and low pressure sides, respectively, A_{yz} is the effective area, Δt is the MD time step, and n_{s} is the number of the MD steps over which the average is taken (we typically use

n_s = 25 000). The factor 2 in the denominator of this equation is due to the fact that since a single mover from the high pressure side to the low pressure side of the flux plane counts both as a deletion on the high pressure side and a creation in the low pressure side, subtracting the net creations of the high pressure side from the low pressure side will result in a double counting of the corresponding flux. The dynamic separation factor is calculated by Eq. (5) as described above.

2.4. Estimation of chemical potentials

Before either GCMC or GCMD simulations, Widom test particle method in *NVT* ensemble is employed to determine the relationship of chemical potentials of the two components with the bulk pressure when fixing composition of mixtures, and with composition of mixtures when fixing bulk pressure at given temperature (here T = 303 K). Simulations start with face centered cubic (FCC) structure, which involves 500 molecules, for the former we fix 105 oxygen molecules and 395 nitrogen molecules and then change their densities, while for the latter we fix their density (ρ^* = 0.01) and then change the ratios of oxygen to nitrogen. Five million configurations are used to reach equilibrium and another five million configurations are summed up to get the system average. Three test insertions of oxygen and nitrogen molecules are performed with the equal probability in each configuration to calculate the corresponding excess chemical potentials.

3. Result and discussion

We first present the results simulated by Widom test particle method, and then discuss those for the binary mixtures by the GCMC and GCMD methods. As described above, the mole fraction of oxygen in the feed mixture is 0.21.

3.1. Chemical potentials

Through Widom test particle method, the relationship of the chemical potentials of the two components with the total system pressures can be obtained. Here the temperature is 303 K and the mole fraction of oxygen is fixed at 0.21 (i.e. $x_{O_2} = 0.21$). The results are plotted in Fig. 3. Generally speaking, the two chemical potential curves are similar. When the pressures approach to zero, they approach to negative infinite. However, the increase of the chemical potentials becomes slower and slower at high pressure. When the system pressure is lower than 15 MPa, these two curves can be expressed well by a logarithmic function given, respectively, by

$$\mu^*_{O_2} = -32.7426 + 2.8058 \ln(p^*) \quad (9a)$$

$$\mu^*_{N_2} = -28.2016 + 2.8492 \ln(p^*) \quad (9b)$$

where the chemical potentials and pressure are reduced by the Lennard–Jones potential parameters of oxygen, i.e. $\mu^* = \mu/\varepsilon_{O_2}$, $p^* = p\sigma^3_{O_2}/\varepsilon_{O_2}$. The relativities of the above two equations are larger than 0.999. But we must point out that at a rather higher pressure, a larger discrepancy will be observed if a logarithmic expression is still used to represent the relation between the reduced chemical potential and pressure. Therefore if we want to obtain the results of membrane processes at the higher pressure, we need to use cubic interpolating spline method by MATLAB software to obtain the corresponding chemical potentials of species i at given bulk pressure and temperature. Fortunately the air is fed through the adsorbent at operating pressure of between 0.4 and 0.8 MPa at ambient temperature in the industrial process of oxygen/nitrogen recovery. Therefore it is unnecessary to use cubic interpolating spline method in this work.

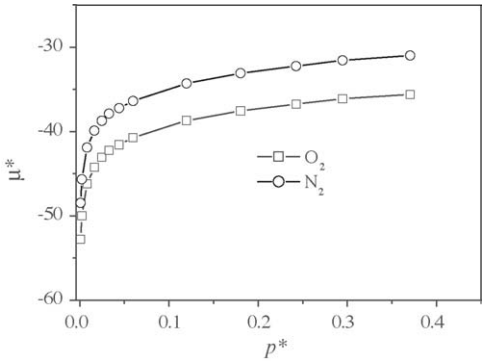

Fig. 3. Reduced chemical potential as a function of the reduced bulk pressure for N_2/O_2 mixture at 303 K. In the bulk phase, the mole fraction of oxygen is fixed at 0.21.

The relationship of reduced chemical potentials of components with mixture composition is also achieved, which will be used to calculate the potential of species at the permeate side, and the results are plotted in Fig. 4. In this case, the reduced total density is fixed at 0.01 and the temperature is 303 K. The average system pressure at the permeate side is about 1.0501 MPa. The analytic expression of chemical potentials can be obtained by fitting the NVT ensemble

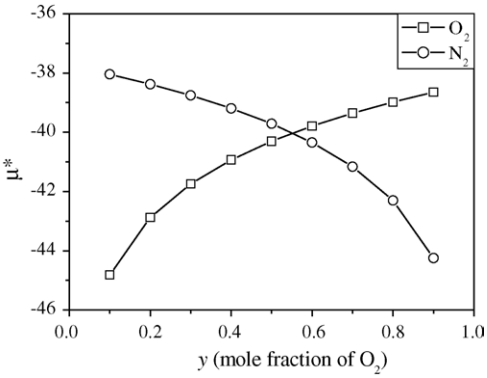

Fig. 4. Reduced chemical potential of species i as a function of the composition for N_2/O_2 mixture at 303 K. The pressure of permeate side is fixed at 1.0501 MPa.

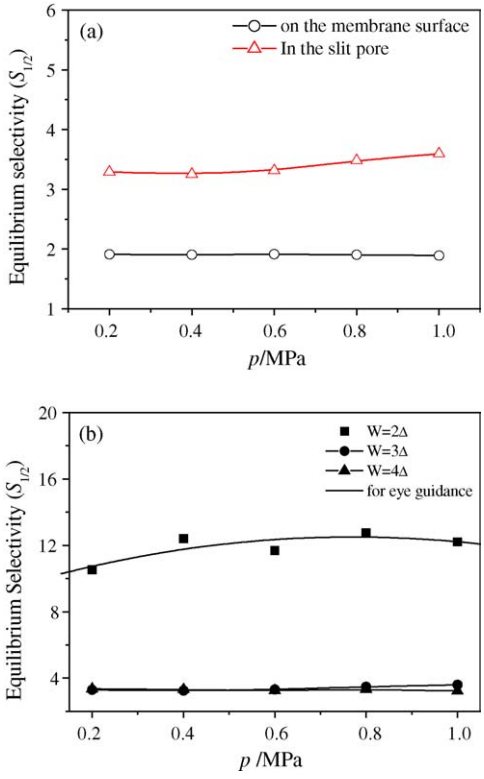

Fig. 5. Equilibrium selectivity of O_2/N_2 as a function of the pressure at 303 K. (a) Selectivity in the pore and on the membrane surface, where the membrane thickness and the pore width are $29L_{cc}$ and 3Δ, respectively. (b) The selectivity in the pore, whose width changes from 2Δ to 4Δ.

simulation data in Fig. 4

$$\mu^*_{O_2} = -38.3532 + 2.8104\ln(x_{O_2}) \quad (10a)$$

$$\mu^*_{N_2} = -37.7478 + 2.8268\ln(1 - x_{O_2}) \quad (10b)$$

Eqs. (10a) and (10b) represent the reduced chemical potentials as a function of the composition for nitrogen and oxygen, respectively. The main purpose of this work is to obtain the more reasonable fluxes and dynamics separation factors. Different purity of product will be achieved when membranes with different pore sizes are used. As discussed above, Eq. (5) shows that product purity is directly related to membrane selectivity. The separation factors from product purity must be consistent with those from permeability and the results simulated by this way can directly compared with those from experiments.

3.2. Equilibrium adsorption and selectivity

After obtaining the relation between chemical potential and the bulk pressure for each component *i* of the gas mixture, we carry out the GCMC simulation to calculate the equilibrium adsorption selectivity of oxygen/nitrogen according to Eq. (3). Fig. 5(a) and (b) present the effect of the bulk pressure p^* on the equilibrium adsorption selectivity of oxygen/nitrogen (S_{O_2/N_2}) in their binary mixtures at 303 K. Here the membrane thickness is $29L_{cc}$ (about 4.118 nm) and the pore width is 2Δ, 3Δ, 4Δ (about 0.67, 1.005, and 1.34 nm), respectively. The mole fraction of oxygen in the bulk phase is set at 0.21. The pore width in Fig. 5(a) is 3Δ. We compare the selectivity on the membrane surface with that in the slit pore and find the selectivity in the pore has a slight enhance with the increase of the bulk pressure, while that out of the pore is unchanged. This indicates that rather high pressure is of no benefit to the separation of oxygen from air, especially when the pore width is rather larger. Fig. 5(b) presents the effect of the bulk pressure on the selectivity in the slit pore under the condition of different pore widths. Results show that when the slit-like pore is very small, e.g. $W = 0.67$ nm, $S_{1/2}$ will slightly increases with the increase of the bulk pressure. This is because that when pore width is large enough, both oxygen and nitrogen molecules can be available to the pore easily and supply the enough sources for the competitive adsorption between them on the pore wall. But when we reduce the pore width, molecules preferentially adsorbed onto the wall will have a stronger resistance to the adsorption of another kind of gas molecules. Since oxygen has a higher value of LJ energy parameter, it will preferentially be adsorbed. In the meantime, to increase the bulk pressure is to increase the opportunity of the pore wall adsorbing oxygen molecules.

Since the values of equilibrium selectivity are larger than unit both on the membrane surface and in the pores as shown in Fig. 5, oxygen should be adsorbed on the membrane wall more easily than nitrogen. To prove our guess, we also investigate the density distributions of oxygen/nitrogen near the membrane surface and in the slit-like pore, respectively. The density distributions of oxygen and nitrogen along *x*-direction out of the pores are plotted in Fig. 6(a). Both oxygen and nitrogen have a strong adsorption on the membrane surface. In addition, the oxygen density is still much lower than that of nitrogen near the membrane surface partially due to that nitrogen has a higher mole fraction in the bulk phase. We must mention that a little progress has been made in the equilibrium adsorption and transport of mixtures through membranes since we consider the membrane thickness as an important factor, which has a strong effect on the adsorption characters and permeability. As shown in Fig. 6(b) and (c), the equilibrium density profiles of mixtures we have obtained are two-dimensional, which is the most different from previous work [2,29,14,30]. We can find from Fig. 6(b) and (c) that the effect of the pore entrance on the density distribution of components is manifest. We only calculate the quarter of the density distribution since the density distribution of components is symmetrical in the slit pore and in order to make the program finish more quickly.

The pore width is a vital factor for membrane separation processes. We investigate the effect of pore width on $S_{1/2}$ at 303 K and 1 MPa. Here the membrane thickness is set at $29L_{cc}$ (about 4.118 nm) and the pore width changes from 2Δ to 6Δ. The simulation results are plotted in Fig. 7,

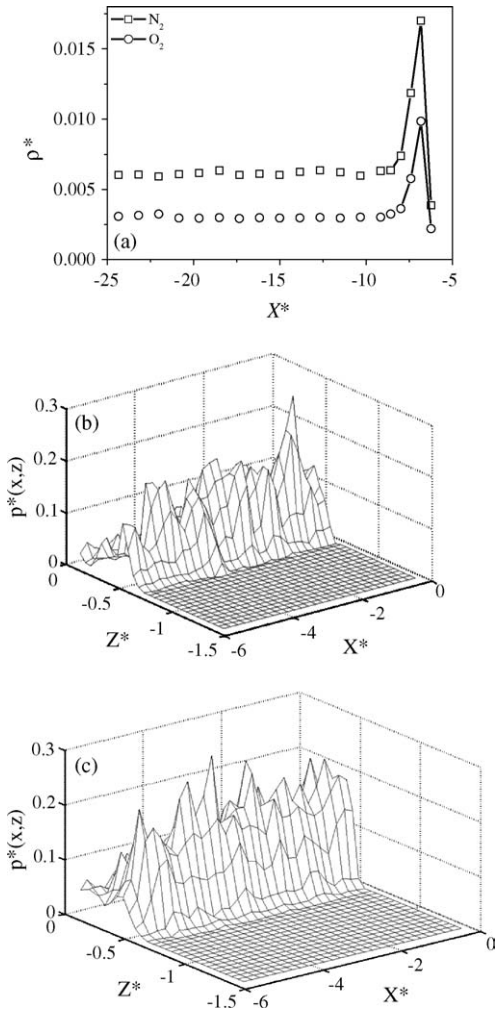

Fig. 6. Density distribution in x and x–z directions for N_2 and O_2 at 303 K and 1 MPa: (a) oxygen and nitrogen along x-direction near the membrane surface, (b) oxygen in the pore and (c) nitrogen in the pore. The membrane thickness and the pore width are $29L_{cc}$ and 3Δ, respectively.

indicating that the smaller the pore size is, the higher the selectivity in the pore. It is also clearly shown that when the pore width is larger than 1.0 nm, the equilibrium selectivity in the pore improves little as pore width decreases, while

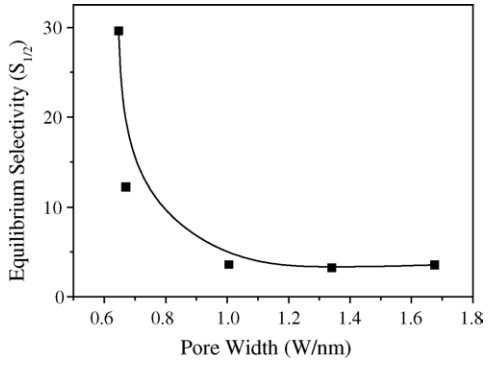

Fig. 7. Effect of the pore width on the equilibrium selectivity of O_2/N_2 at 303 K and 1 MPa. The membrane thickness is $29L_{cc}$.

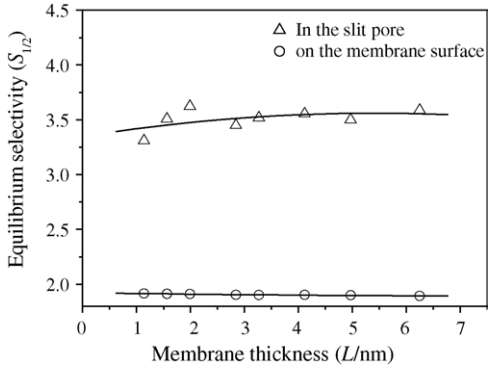

Fig. 8. Effect of the membrane thickness on the equilibrium selectivity of O_2/N_2 at 303 K and 1 MPa. The pore width is 5Δ and the solid lines are for eye guidance.

it enhances apparently when the pore width is smaller than 1.0 nm. This is because all molecules are considered as soft spheres with an effective hard-core diameter in the simulations. When the pore is very small, e.g. $W = 0.67$ nm, it can easily hold the smaller molecules like oxygen but hardly for the bigger nitrogen molecules. Subsequently most of oxygen molecules enter the slit pore and the selectivity becomes high. But when the pore is wider, e.g. $W = 1.005$–2.01 nm, molecules of two species can easily enter the pore. We can conclude that molecular sieving plays a more important role than adsorption in the efficient separation of O_2/N_2 gas mixture.

We also study the effect of the membrane thickness on the equilibrium selectivity of O_2/N_2 both on the membrane surface and in the slit pore at 303 K and 1 MPa. Here the membrane is with a width of 5Δ (about 1.675 nm). The results are plotted in Fig. 8. In fact, the true thickness of the membranes is difficult to measure or even to define since there are supported membranes and thus the definition of their true thickness is ambiguous. In the separation process the dense layer coated is effective, which is named separation layer, and contains the main resistance of membrane. Therefore the membranes simulated here refer to the dense layers coated and the thickness here is effective thickness.

Fig. 8 reveals that the membrane thickness has a slight effect on the equilibrium selectivity of O_2/N_2 gas mixtures. When the membrane thickness increases from 1.136 to 6.248 nm, $S_{1/2}$ on the surface is almost unchanged, while that in the pore increases a little from 3.31 to 3.59. Because in the steele's 10-4-3 potential model, pore walls are considered as two infinite smooth flats, simulation results will show that the membrane thickness has no effect on the selectivity of gas mixture. Therefore when we study the equilibrium characters of fluids, the steele's potential model may be applied to accelerate calculations because the effect of membrane thickness is little. But when we study the dynamical characters of fluids, there will be an discrepancy if the steele's potential model is employed.

3.3. Flux and dynamic separation factor

Equilibrium properties of fluids can give us insight into the deeply understanding membrane process, but non-equilibrium dynamic characters are more significant for the membrane separation. Consequently, we investigate the flux and dynamic separation factor of gas mixture using DCV-GCMD developed by Heffelfinger and Swol [16] in this work.

Just as the described in Section 2.3 of this work, we think the composition in the permeate side is different from that in the feed side and has an unnegligible effect on the transport properties of fluids. Therefore, we obtain the flux of fluids through membranes using iteration method. In the previous work [5,10], the pressure in the permeate side, p^{L}, is usually set at zero to calculate the permeability and dynamic separation factor. In Fig. 9(b) we present what happens in the flux of fluids when the iteration method is not applied. Here membrane thickness is $14L_{cc}$, the pore width is ranging from 2Δ to 6Δ, the pressure gradient is 1 MPa, and the pressure in the permeate side is 1.0501 MPa by iteration method and zero by non-iteration method. The simulated results using the iteration and non-iteration methods are shown in Fig. 9(a) and (b), respectively. From the two figures one can see that the trends of the flux as a function of pore width are similar in the two cases, but the absolute values of fluxes of both oxygen and nitrogen are different. The fluxes decrease apparently when the iteration method is used, showing that the condition in the permeate side has a great effect on the fluid permeation.

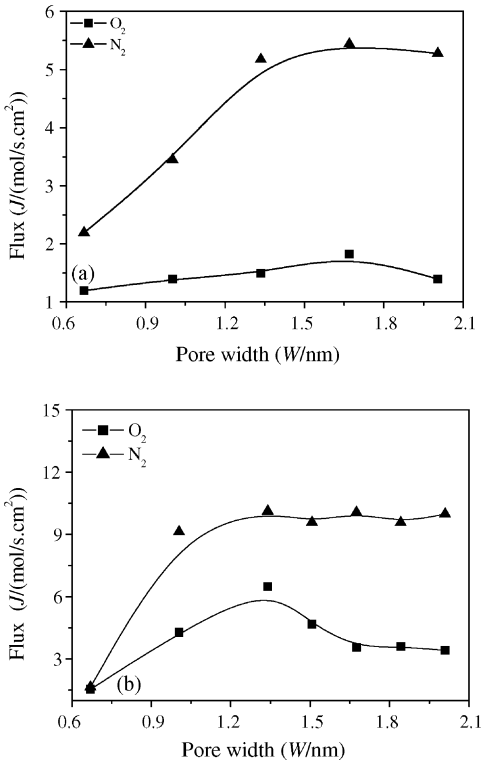

Fig. 9. Effect of the pore width on the fluxes of oxygen/nitrogen through membranes from (a) the iteration method and (b) the non-iteration method. The membrane thickness is $14L_{cc}$, and the pressure gradient is 1 MPa. The permeate side pressures p^{L} are 0 and 1.0501 MPa in the non-iteration and iteration calculations, respectively.

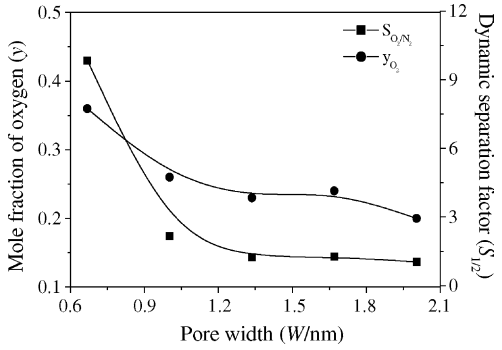

Fig. 10. Product purity and dynamic separation factor vs. the pore width for N_2/O_2 gas mixtures at 303 K. The membrane thickness is $14L_{cc}$, the pressure gradient is 1 MPa, and the permeate side pressure is fixed at 1.0501 MPa.

The product purity and dynamic separation factor as functions of the pore width is plotted in Fig. 10. The simulation conditions in this figure are the same as those in Fig. 9(a). Fig. 10 shows that the pore width has an important effect on the oxygen concentration in the permeate side of membranes y_1 and their dynamic separation factor $S_{1/2}$. Both y_1 and $S_{1/2}$ decrease with the increase of the pore width. When the pore width is up to 6Δ, the oxygen concentration is almost equal to that in the feed side, e.g. the membrane lost its separation function. In addition, the dynamic separation factors are rather lower than the equilibrium separation factors, especially when the pore is very small. For example, when the pore width is down to 2Δ, the equilibrium selectivity is up to 29.62 while the dynamic separation factor is only 9.85. This indicates that the selective adsorption does not play a dominant role in the non-equilibrium transport properties of oxygen/nitrogen gas mixture through carbon membranes. It should be pointed out that since our membrane model is highly idealized, even the dynamic separation factors will not be attained in the real separations because of various adverse factors including back-diffusion, non-ideal membranes, concentration polarization and surface flow phenomena.

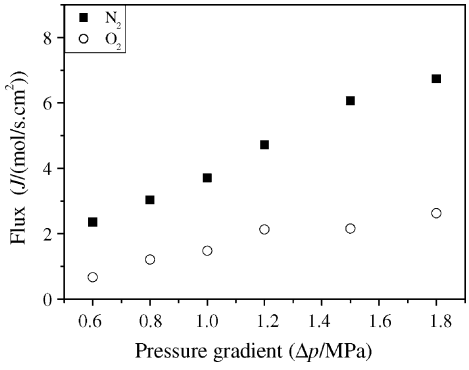

Fig. 11. Fluxes of oxygen and nitrogen through membranes ($L = 14L_{cc}$, $W = 3\Delta$) vs. the pressure gradient at 303 K.

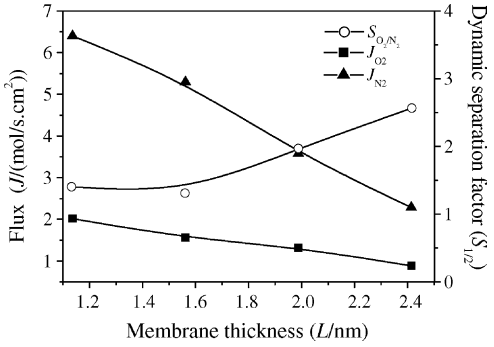

Fig. 12. Effect of membrane thickness on the transport and separation of oxygen/nitrogen in carbon membranes. The pore width is 3Δ, the temperature is 303 K, and the feed and permeate side pressures are 2.0501 and 1.0501 MPa, respectively.

Fig. 11 shows the effect of the pressure gradient on the flux of oxygen and nitrogen through carbon membranes at 303 K, where the membrane thickness and pore width are $14L_{cc}$ and 3Δ, respectively. The permeate side pressure is fixed at 1.0501 MPa and the feed pressure changes ranging from 1.6501 to 2.8501 MPa. From the simulation results we can conclude that the increase of the pressure gradient results in the improvement of the fluxes of both oxygen and nitrogen in consistence with that in real experiments.

Just as described above, one advance in this work is that we use a novel two-dimensional slit pore instead of one-dimensional pore for carbon membranes, which makes it possible to study the effect of membrane thickness on the fluid characters in carbon membranes, and now we discuss the effect of membrane thickness on the transport and separation of oxygen and nitrogen in carbon membranes. Fig. 12 displays that it manifestly impacts on the fluxes of two species and the dynamic separation factors. Here the pore width is set at 3Δ, temperature is 303 K, the feed pressure and the permeate side pressure are 2.0501 and 1.0501 MPa, respectively. The fluxes of both oxygen and nitrogen go down with the increase of the membrane thickness, and that of nitrogen descends more sharply than that of oxygen. This is easily explained by the knowledge of membrane resistance. An alternative expression [5] for the permeation rate may be a function of the permeation resistance and a driving force:

$$\text{flux} = \frac{\text{driven-force}}{\text{resistance}}$$

Where the driving force can be the difference of density, pressure or chemical potential, the resistance is consisting of the sum of resistances of the other fluid molecules and membrane, the pore entrance, the inside diffusion and the pore exit. The membrane resistance is directly related with the membrane thickness, especially with the effective thickness of the dense layer coated.

4. Conclusions

We have described the simulations on the permeation and adsorption selectivity of O_2/N_2 binary gas mixture through the carbon membranes with slit-like pores at 303 K. In our study the mole fraction of oxygen in the feed side is fixed at 0.21, and the classic GCMC and DCV-GCMD methods developed by Heffelfinger and Swol [16] are employed.

In addition, we have proposed a new approach with iterations to calculate the flux of species and the dynamic separation factors for binary gas mixtures. The greatest advantage of this method is its ability of directly corresponding to real experimental conditions. And the results by his method are more reasonable due to deducing of exact expression for separation factors. The shortcomings of this method are its time-consuming comparing with that method without iterations, and its stability also needs to be improved further.

Although the membrane model used in this work is still highly idealized, considering the pore wall as the pure graphite layers, it makes some advances compared with previous work because of the consideration of longitudinal structure and the thickness of carbon membranes. The simulation results indicate that for O_2/N_2 gas mixture in carbon membranes both their dynamic separation factors and equilibrium selectivity are not mainly dependent on the selective adsorption of gases but molecular sieving. As pore width increases, the fluxes of both oxygen and nitrogen increase but the oxygen concentration of low-pressure side gases decreases. Especially for the rather small pores, this trend becomes more obvious. The membrane thickness and the bulk pressure affect slightly on the equilibrium selectivity but greatly on the flux and dynamic separation factor of binary gas mixtures. In this work we also find that the highest purity of oxygen in permeate side at 303 K and 1 MPa for the pressure gradient is less than 0.4, where the pore width has been down to 2Δ. If the higher purity oxygen is expected, the carbon membranes should be modified with some functional groups.

Acknowledgement

The research is supported by the National Basic Research Program of China under Grant No. 2003CB615700.

Nomenclature

A	area (m^2)
ΔE	change of energy
J	permeation flux (mol/m^2 s)
k	Boltzmann's constant (J/K)
L	membrane thickness (m)
L_{cc}	separation distance between two nearest carbon in the same graphite layer (m)
N	number of gas molecule

p	pressure (Pa)
P	permeance (mol/m^2 s Pa)
$\hat{P}$	accepted probability in GCMC simulations
R	ratio of the number of GCMC in control volumes to the number of MD
S	separation factor
Δt	time step (s)
T	absolute temperature (K)
V	volume (m^3)
W	pore width (nm)
x	mole fraction of gas in feed side
y	mole fraction of gas in permeate side
Z	absolute activity (m^{-3})

Greek letters

Δ	distance between two nearest graphite layer (nm)
ε	Lennard–Jones energy parameter (J)
Λ	de Broglie thermal wavelength (m)
μ	chemical potential (J/mol)
ρ	number density (nm^{-3})
σ	Lennard–Jones size parameter (nm)

Subscripts

b	bulk
ev	ensemble average
i, j	component i and j
s	step
1	oxygen
2	nitrogen

Superscripts

H	high pressure region of simulation box
L	low pressure region of simulation box
*	reduced unit
+	insertion in GCMC simulation
−	deletion in GCMC simulation

References

[1] J. Zhou, W.C. Wang, Adsorption and diffusion of supercritical carbon dioxide in slit pores, Langmuir 16 (2000) 8063.

[2] Z.M. Tan, K.E. Gubbins, Adsorption in carbon micropores at supercritical temperature, J. Phys. Chem. 94 (1990) 6061.

[3] L.F. Xu, M.G. Sedigh, T.T. Tsotsis, M. Sahimi, Nonequilibrium molecular dynamics simulation of transport and separation of gases in carbon nanopores. II. Binary and ternary mixtures and comparison with the experimental data, J. Chem. Phys. 112 (2000) 910.

[4] J.M.D. MacElroy, M.J. Boyle, Nonequilibrium molecular dynamics simulation of a model carbon membrane separation of CH_4/H_2 mixture, Chem. Eng. J. 74 (1999) 85.

[5] S. Furukawa, T. Nitta, Non-equilibrium molecular dynamics simulation studies on gas permeation across carbon membranes with different pore shape composed of micro-graphite crystallites, J. Membr. Sci. 178 (2000) 107.

[6] T. Ohba, D. Nicholson, K. Kaneko, Temperature dependence of micropore filling of N_2 in slit-shaped carbon micropores: experiment and grand canonical Monte Carlo simulation, Langmuir 19 (2003) 5700.

[7] L.F. Xu, M.G. Sedigh, M. Sahimi, Nonequilibrium molecular dynamics simulation of transport of gas mixtures in nanopores, Phys. Rev. Lett. 80 (1998) 3511.

[8] J. Lin, S. Murad, A computer simulation study of the separation of aqueous solutions using thin zeolite membranes, Mol. Phys. 99 (2001) 1175.

[9] G.Z. Cao, Y.F. Lu, L. Delattre, J. Brinker, G.P. Lopez, Amorphous silica molecular sieving membranes by sol–gel processing, Adv. Mater. 8 (1996) 588.

[10] H. Takaba, K. Mizukami, M. Kubo, A. Fahmi, A. Miyamoto, Permeation dynamics of small molecules through silica membranes: molecular dynamics study, AIChE J. 44 (1998) 1335.

[11] T. Yoshioka, T. Tsuru, M. Asaeda, Molecular dynamics studies on gas permeation properties through microporous silica membranes, Sep. Purif. Technol. 25 (2001) 441.

[12] P.L. Pohl, G.S. Heffelfinger, D.M. Smith, Molecular dynamics computer simulation of gas permeation in thin silicalite membranes, Mol. Phys. 89 (1996) 1725.

[13] M.P. Allen, D.J. Tildesley, Computer Simulation of Liquids, Clarendon Press, Oxford, 1987.

[14] M. Firouzi, T.T. Tsotsis, Nonequilibrium molecular dynamics simulations of transport and separation of supercritical fluid mixtures in nanoporous membranes. I. Results for a single carbon nanopore, J. Chem. Phys. 119 (2003) 6810.

[15] A. Papadopouloou, E.D. Becker, M. Lupkowski, F. vanSwol, Molecular dynamics and Monte Carlo simulations in the grand canonical ensemble: local versus global control, J. Chem. Phys. 98 (1993) 4897.

[16] G.S. Heffelfinger, F.V. Swol, Diffusion in Lennard–Jones fluids using dual control volume grand canonical molecular dynamics simulation (DCV-GCMD), J. Chem. Phys. 100 (1994) 7548.

[17] S. Sunderrajan, C.K. Hall, B.D. Freeman, Estimation of mutual diffusion coefficients in polymer/penetrant systems using nonequilibrium molecular dynamics simulations, J. Chem. Phys. 105 (1996) 1621.

[18] D.M. Ford, E.D. Glandt, Molecular simulation study of the surface barrier effect. Dilute gas limit, J. Phys. Chem. 99 (1995) 11543.

[19] M. Firouzi, K.M. Nezhad, T.T. Tsotsis, M. Sahimi, Molecular dynamics simulations of transport and separation of carbon dioxide-alkane mixtures in carbon nanopores, J. Chem. Phys. 120 (2004) 8172.

[20] Y.G. Seo, G.H. Kum, N.A. Seaton, Monte Carlo simulation of transport diffusion in nanoporous carbon membranes, J. Membr. Sci. 195 (2002) 65.

[21] A.M. Vieira-Linhares, N.A. Seaton, Nonequilibrium molecular dynamics simulation of gas separation in a microporous carbon membrane, Chem. Eng. Sci. 58 (2003) 4129.

[22] L.F. Xu, M. Sahimi, T.T. Tsotsis, Nonequilibrium molecular dynamics simulations of transport and separation of gas mixtures in nanoporous materials, Phys. Rev. E 62 (2000) 6942.

[23] W.A. Steele, The Interaction of Gases with Solid Surfaces, Pergamon Press, Oxford, 1974.

[24] P.I. Pohl, G.S. Heffelfinger, Massively parallel molecular dynamics simulation of gas permeation across porous silica membranes, J. Membr. Sci. 155 (1999) 1.

[25] H. Takaba, E. Matsuda, B.N. Nair, S. Nakao, Molecular modeling of gas permeation through an amorphous microporous silica membrane, J. Chem. Eng. Jpn. 35 (2002) 1312.

[26] K. Lee, S.B. Sinnott, Computational studies of non-equilibrium molecular transport through carbon nanotubes, J. Phys. Chem. B 108 (2004) 9861.

[27] J.M.D. MacElroy, S.P. Friedman, N.A. Seaton, On the origin of transport resistances within carbon molecular sieves, Chem. Eng. Sci. 54 (1999) 1015.

[28] M.C. Porter, Handbook of Industrial Membrane Technology, Noyes Publications, New Jersey, 1990.

[29] S. Murad, P. Ravi, J.G. Powles, A computer simulation study of fluids in model slit, tubular, and cubic micropores, J. Chem. Phys. 98 (1993) 9771.
[30] S.K. Bhatia, D. Nicholson, Molecular transport in nanopores, J. Chem. Phys. 119 (2003) 1719.
[31] K. Kaneko, R.F. Cracknell, D. Nicholson, Nitrogen adsorption in slit pores at ambient temperatures: comparison of simulation and experiment, Langmuir 10 (1994) 4606.
[32] M.J. Bojan, W.A. Steele, Interactions of diatomic molecules with graphite, Langmuir 3 (1987) 1123.